ChemComm

ROYAL SOCIETY OF CHEMISTRY

COMMUNICATION

View Article Online
View Journal | View Issue

Cite this: *Chem. Commun.*, 2024, **60**, 10954

Received 28th June 2024,
Accepted 5th September 2024

DOI: 10.1039/d4cc03184a

rsc.li/chemcomm

Proximity-induced FRET and charge-transfer between quantum dots and curcumin enable reversible thermochromic hybrid polymeric films†

Jefin Parukoor Thomas,[ac] R. B. Amal Raj,[a] G. Virat,[ac] Amarjith V. Dev,[bc] Chakkooth Vijayakumar [bc] and E. Bhoje Gowd *[ac]

This study introduces a novel strategy for developing reversible thermochromic fluorescent films by precisely controlling the nanoscale proximity of boron nitride quantum dots and curcumin molecules within a poly(3-hydroxybutyrate) matrix. The synergistic interaction and Förster resonance energy transfer between these fluorophores result in an energy transfer efficiency of ~94%. This approach enables tunable color changes in response to temperature variations, governed by the segmental mobility of polymer chains. Practical applications of these films as temperature sensors for water bottles and electronic devices are demonstrated, highlighting their potential in temperature monitoring, smart packaging, and thermal management systems.

Thermochromic materials, which change color in response to temperature, have shown remarkable potential in developing fluorescent thermometers, temperature labels, and smart packaging materials.[1–7] These materials are often embedded in polymer matrices, where color changes occur through various mechanisms, including chemical structure alterations, phase transformations, and additive-assisted interactions.[5–15] The emission behavior can be modulated by annealing the glassy systems above the glass transition temperature (T_g) or by crystallizing the semicrystalline polymers, where the aggregation of fluorophores can be meticulously controlled.[4,10–14,16] Förster resonance energy transfer (FRET) has emerged as an efficient method for modulating the thermochromic behavior in polymer-based systems, relying on the spatial proximity of donor and acceptor fluorophores.[6,8,17–20]

Various fluorophores are used in FRET applications, including organic molecules, inorganic nanoparticles, and fluorescent proteins.[13,14,20–22] Quantum dots (QDs) are particularly effective donors due to their broad UV absorption, high quantum yields, and tunable, narrow emission spectra.[21,23–26] Despite the promising applications of thermochromic materials, there remains a significant gap in understanding the precise modulation of thermochromic behavior in multi-component systems through FRET.[20] Earlier research primarily focuses on FRET systems with limited consideration of the polymer matrix's role, leaving the potential of integrating FRET pairs with responsive polymer matrices largely unexplored.[21–24,27]

This study focuses on boron nitride quantum dots (BNQDs), a type of heavy metal-free, two-dimensional QDs that offer unique advantages for FRET applications. BNQDs address environmental and health concerns associated with conventional QDs while exhibiting excellent biocompatibility, superior chemical stability, and unique optical properties. While BNQDs present some synthesis challenges, their benefits outweigh these difficulties for the specific requirements of this research. These materials, with their unique luminescence properties and ease of functionalization, present an exciting opportunity for developing advanced thermochromic systems.[28–30] However, the challenge lies in achieving controlled and efficient FRET within these systems to harness their full potential for practical applications.

In this work, we developed reversible thermochromic films by integrating polyethylene glycol-modified hexagonal boron nitride QDs (PQDs) as energy donors and curcumin (Cur) (1,7-bis(4-hydroxy-3-methoxyphenyl)-1,6-heptadien-3,5-dione) as acceptors within a biodegradable poly(3-hydroxybutyrate) (PHB) matrix. The interactions between PQDs and Cur molecules are specifically controlled by the segmental mobility of polymer chains, enabling tunable color changes. These hybrid films exhibit excellent reversible thermochromism under both daylight and UV light, demonstrating potential for real-life applications in temperature monitoring and smart packaging.

Hybrid films were fabricated using PQDs (lateral size of 2–4 nm; See Fig. S1–S4 (ESI†) for preparation and characterization) and Cur molecules (Fig. 1a). The preparation involved adding Cur solution to PHB in chloroform, followed by the

[a] *Materials Science and Technology Division, CSIR-National Institute for Interdisciplinary Science and Technology, Trivandrum 695 019, Kerala, India. E-mail: bhojegowd@niist.res.in*

[b] *Chemical Sciences and Technology Division, CSIR-National Institute for Interdisciplinary Science and Technology, Trivandrum 695 019, Kerala, India*

[c] *Academy of Scientific and Innovative Research (AcSIR), Ghaziabad 201 002, India*

† Electronic supplementary information (ESI) available. See DOI: https://doi.org/10.1039/d4cc03184a

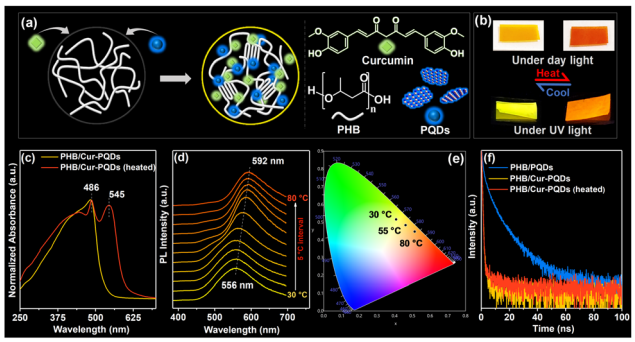

Fig. 1 (a) Schematic of thermochromic film fabrication. (b) Photographs of hybrid film under daylight and UV light. (c) UV-visible absorption spectra of PHB/Cur-PQDs (with 6 wt% PQDs) before and after heating. (d) Temperature-dependent PL emission spectra of PHB/Cur-PQDs (6 wt% of PQDs). (e) CIE chromaticity plot for color coordinates displaying the color change with temperature. (f) Time-resolved fluorescence decay curves of PHB/PQDs, PHB/Cur-PQDs and PHB/Cur-PQDs (after heating) (6 wt% of PQDs).

addition of PQDs (5 and 10 mL) using a solution blending method. Films were dried under high vacuum at 45 °C for 48 h to remove residual solvents. A control experiment with PHB/Cur film prepared using dimethylformamide (DMF) showed no color change upon heating, confirming the absence of DMF-curcumin interactions (Fig. S5, ESI†). The PQDs content in the hybrid film was estimated to be 6 and 12 wt%, respectively. The resulting films exhibited a yellow color at room temperature, changing to reddish-orange when heated, observable under both UV light and daylight (Fig. 1b).

UV-visible absorption spectra showed bands at 486 nm for as-cast films, with a new band at 545 nm in heated films (Fig. 1c). The new band likely results from charge transfer (CT) complex formation between PQDs and Cur molecules.[31] This change in absorbance due to CT complex formation contributes to the color change observable under visible light, while the FRET process (as discussed later) primarily affects the emission color seen under UV light. The interplay of these mechanisms produces thermochromic behavior visible under both conditions. Similar results were observed with higher PQDs (up to 12 wt%) and unmodified QDs loadings (Fig. S6a and b, ESI†). Heating enhances the mobility and diffusion of polymer chains and fluorophores, facilitating the formation of CT complexes.

The PL emission spectra of PQDs showed effective overlap with the absorption band of PHB/Cur (Fig. S7, ESI†), indicating the possibility of FRET from PQDs (donor) to Cur molecules (acceptor). Temperature-dependent photoluminescence (PL) emission spectra for hybrid films with 6 wt% PQDs revealed a clear red shift (556 to 592 nm) as the temperature increased from 30 to 80 °C (Fig. 1d; excitation at 365 nm). No change was observed up to 45 °C, but beyond 50 °C, the emission wavelength shifted with increasing temperature, accompanied by an enhancement in peak intensity and a decrease in the full width at half maximum. This behavior can be explained by the polymer's glass transition temperature (T_g) and chain mobility. The T_g of PHB is low, around 3 °C. Just above T_g, only micro-Brownian motion of polymer chain segments occurs, which is insufficient to cause significant changes in fluorophore arrangement. As the temperature increases well above T_g (around 50 °C and higher), the polymer chains gain much more vigorous mobility. This enhanced mobility facilitates the diffusion and reorientation of Cur molecules and PQDs within the PHB matrix, allowing the fluorophores to achieve the proximity required for forming charge transfer (CT) complexes. The gradual color change may also be partly attributed to the time-dependent reorganization of fluorophores within the polymer matrix.

Similar red shifts were observed with higher loadings of PQDs (12 wt%; Fig. S8a, ESI†) and unmodified QDs (Fig. S8b, ESI†). However, films with unmodified QDs exhibited an additional shoulder peak at 500 nm, attributed to aggregated curcumin molecules, signifying the necessity of QDs modification. Notably, PHB/Cur and PHB/PQDs alone did not show any change in PL emission with temperature (Fig. S8c and d, ESI†, respectively), confirming that the red-shift in hybrid films is primarily due to the formation of CT complexes and FRET between PQDs and Cur molecules. The CIE chromaticity diagram confirmed the fluorescence color change from yellow to reddish-orange with the increase in temperature (Fig. 1e).

Time-resolved fluorescence measurements using time-correlated single-photon counting (TCSPC) were conducted to further investigate the FRET process (Fig. 1f; excitation at 331 nm and emission monitored at donor emission maximum). The fluorescence decay profile of PHB/PQDs film was fitted with a triexponential function, indicating three emissive species (Table S1, ESI†).[27] In PHB/PQDs, the higher lifetime (τ_2 = 12.2 ns) suggests trapped electrons in PQDs defects, while faster decay (τ_1 = 3.5 ns) indicates intrinsic excitonic recombination. A shorter decay (τ_3 = 0.4 ns) likely represents energy transfer between PQDs, consistent with previous reports on polymer/QDs studies.[27,32,33] Adding Cur molecules to PHB/PQDs significantly decreased average fluorescence decay time ($\langle\tau\rangle$ = 0.07 ns), confirming nonradiative energy transfer from PQDs to Cur.

$$E = 1 - \frac{\tau_{DA}}{\tau_D}$$

The FRET efficiency was calculated using the above equation,[14,21] where τ_{DA} and τ_D denote the lifetime of the donor in the presence and absence of the acceptor, respectively. An efficiency of 94% was obtained for the as-cast PHB/Cur-PQDs hybrid film. The heated hybrid film showed a slightly higher average lifetime ($\langle\tau\rangle$ = 0.17 ns) and reduced FRET efficiency (87%), likely due to CT complexes formation. This decrease in FRET efficiency upon heating, despite the presumed shorter donor–acceptor distance, can be attributed to several factors. The formation of CT complexes may alter the spectral overlap between donor emission and acceptor absorption. Additionally, increased mobility of polymer chains and fluorophores at higher temperatures creates a more dynamic system with fluctuating donor–acceptor distances and orientations. Changes in the local environment due to polymer reorganization may also affect the quantum yield of the donor or the absorption coefficient of the acceptor. These factors collectively contribute to the observed decrease in FRET efficiency.

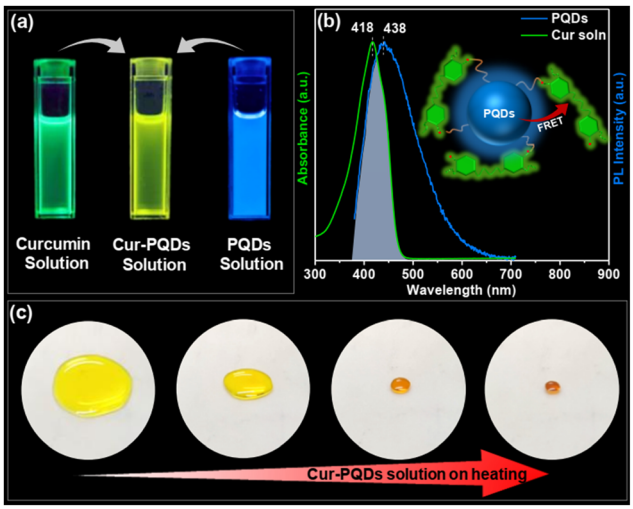

Fig. 2 (a) Digital images of Cur, Cur-PQDs, and PQDs solutions under UV light. (b) Spectral overlap of absorbance of Cur solution and emission band of PQDs (inset showing the FRET between PQDs and Cur molecules). (c) Photographs displaying the visual color change of Cur-PQDs solution on heating.

To investigate interactions and FRET between PQDs and Cur molecules, solution-state PL emission was analyzed. A clear red shift in the PL emission spectra was observed when PQDs were added to the Cur solution (Fig. S9, ESI†), with the emission color changing to yellow under UV light (Fig. 2a). The PL emission spectrum of PQDs showed adequate overlap with the absorption spectrum of the Cur solution (Fig. 2b), fulfilling a key requirement for FRET. While dilute Cur-PQDs solution showed no temperature-dependent changes in emission wavelength (Fig. S10a, ESI†), evaporating the solvent by heating caused a visible color change from yellow to red under daylight (Fig. 2c and Movie S1, ESI†). This demonstrates that proximity between PQDs and Cur is crucial for formation of CT complexes and FRET.[34]

PL emission spectra of concentrated Cur-PQDs solution (Fig. S10b, ESI†) at room temperature showed a change in emission wavelength compared to dilute solution (starting solution in Fig. 2c). This is likely due to restricted mobility of fluorophores in the confined space and the enhanced interactions between solutes resulting from their increased proximity in concentrated solutions, especially as the solvent evaporates during heating, promoting the formation of CT complexes. Control experiments using PHB/PQDs and PHB/Cur solutions were carried out independently, and no color change was observed in both the cases upon heating (Fig. S11, ESI†). These experiments suggested that the proximity of both PQDs and Cur is essential for the observed color change.

Solution-state studies helped to elucidate the color change mechanism in PHB/Cur-PQDs hybrid films. Fig. 3 illustrates the arrangement of fluorophores within the polymer matrix and the reversible thermochromic behavior. PHB is a semicrystalline polymer, and the solvent-cast film crystallizes into the α form.[35] In the PHB/Cur film, Cur resides in the amorphous phase, produces green emission (528 nm; Fig. 3a). In the PHB/Cur-PQDs hybrid film, both Cur and PQDs occupy the

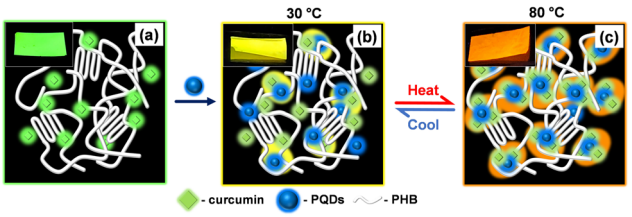

Fig. 3 Schematic representation showing the mechanism of reversible thermochromic behavior of the film (a) PHB-Cur film, (b) PHB/Cur-PQDs hybrid film and (c) PHB/Cur-PQDs film after heating above 50 °C.

amorphous region at 30 °C (Fig. 3b), causing a red-shift in PL emission to 556 nm and changing the film color to yellow. Heating well above the T_g (~3 °C) of PHB (almost 50 °C higher to T_g) increases polymer chain mobility in the amorphous region, allowing diffusion and orientation of Cur and PQDs (Fig. 3c). This facilitates CT complex formation, further red-shifting emission to 592 nm and changing the film color to reddish-orange. Small-angle X-ray scattering (Fig. S12a–c, ESI†) showed decreased amorphous layer thickness (5.2 to 3.5 nm) on heating, indicating improved fluorophore proximity.[36] Temperature-dependent FTIR spectra (Fig. S13a–e, ESI†) confirmed Cur-PQDs interactions through changes in O–H stretching (3750–3200 cm^{-1}) and C=C stretching (1540–1480 cm^{-1}) regions.

Upon cooling to room temperature, the PHB/Cur-PQDs hybrid film gradually reverts to its original yellow color over several hours, demonstrating a slow, reversible thermochromic behavior. This phenomenon is linked to the T_g of the polymer. Heating increases polymer chain mobility, allowing PQDs and Cur molecules to move closer to form CT complexes, resulting in a reddish-orange color. The change in emission wavelength is due to the altered HOMO–LUMO energy gap from CT complex formation.[34] As the T_g of PHB (~3 °C) is below the room temperature (30 ± 3 °C), polymer chains remain mobile during aging, gradually achieving a steady state. This process disturbs the CT complexes, causing the film to return to its original yellow color.

To further confirm the influence of T_g on the reversible thermochromic behavior, heated samples were stored at two different temperatures. One sample was placed at 30 ± 3 °C (well above the T_g of the polymer) and the other was kept inside the freezer at −10 ± 2 °C (below the T_g of the polymer) for 4 h. Fig. S14 (ESI†) shows the photographs of the film before and after the experiment. The sample kept in the freezer did not show any noticeable color change (remaining reddish orange), whereas the room-temperature aged sample reverted to its original color (yellow) because of the chain relaxation of the polymer at room temperature.

To demonstrate real-life applications, the thermochromic films were used as temperature sensor labels for water bottles (Fig. 4). A small piece of hybrid film placed on a glass bottle changed color from yellow to reddish-orange within 3 min when hot water (~75 °C) was poured in (Movie S2, ESI†). The color change was visible under both daylight and UV light. The film can also be used to monitor overheating in electronic devices during charging. Fig. S15 and 16 (ESI†) shows the film's

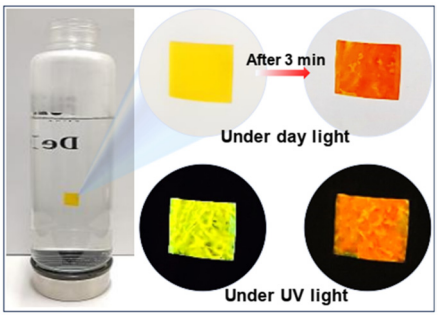

Fig. 4 Photographs of reversible thermochromic film as temperature sensors for hot water bottles under daylight and UV light.

color change when a phone overheats, detectable under both daylight and UV light.

In conclusion, we have fabricated reversible thermochromic hybrid films by integrating PEG-modified boron nitride quantum dots and curcumin within a poly(3-hydroxybutyrate) matrix. The proximity of these fluorophores facilitates efficient FRET, resulting in tunable color changes with temperature. The segmental mobility of polymer chains governs the reversible thermochromic behavior by controlling fluorophore mobility and charge transfer complex formation. This work demonstrates a novel strategy for developing advanced thermochromic materials and provides insights into the role of polymer glass transition temperature in modulating this behavior. The practical applications of these films as temperature sensors highlight their potential in temperature monitoring, smart packaging, and thermal management systems. This research opens avenues for exploring multi-component systems in developing responsive and functional materials with tailored optical properties.

The authors thank Dr Karunakaran Venugopal and Mr Kiran Mohan for PL, lifetime, and TEM measurements. Jefin thanks Dr Lakshmi V. for non-technical support. Authors acknowledge CSIR FTT-FTC/03/05/IMD/2023 for financial support. Jefin thanks UGC, New Delhi for financial support (201610099835).

Data availability

The authors confirm that the data supporting the findings of this article is given within this article and the ESI.†

Conflicts of interest

There are no conflicts to declare.

Notes and references

1 K. Sone and Y. Fukuda, in *Inorganic Thermochromism*, ed. K. Sone and Y. Fukuda, Springer Berlin Heidelberg, Berlin, Heidelberg, 1987, pp. 104–131.
2 C. E. Sing, J. Kunzelman and C. Weder, *J. Mater. Chem.*, 2009, **19**, 104–110.
3 F. Azizian, A. J. Field, B. M. Heron and C. Kilner, *Chem. Commun.*, 2012, **48**, 750–752.
4 A. Julià López, D. Ruiz-Molina, K. Landfester, M. B. Bannwarth and C. Roscini, *Adv. Funct. Mater.*, 2018, **28**, 1801492.
5 A. Pucci and G. Ruggeri, *J. Mater. Chem.*, 2011, **21**, 8282–8291.
6 A. Seeboth, D. Lötzsch, R. Ruhmann and O. Muehling, *Chem. Rev.*, 2014, **114**, 3037–3068.
7 M. Babazadeh-Mamaqani, M. Mohammadi-Jorjafki, S. Alipour-Fakhri, H. Mardani and H. Roghani-Mamaqani, *Macromolecules*, 2023, **56**, 5843–5853.
8 A. Seeboth, D. Lötzsch and R. Ruhmann, *J. Mater. Chem. C*, 2013, **1**, 2811–2816.
9 A. Pucci, R. Bizzarri and G. Ruggeri, *Soft Matter*, 2011, **7**, 3689–3700.
10 B. R. Crenshaw and C. Weder, *Adv. Mater.*, 2005, **17**, 1471–1476.
11 M. Kinami, B. R. Crenshaw and C. Weder, *Chem. Mater.*, 2006, **18**, 946–955.
12 B. R. Crenshaw, J. Kunzelman, C. E. Sing, C. Ander and C. Weder, *Macromol. Chem. Phys.*, 2007, **208**, 572–580.
13 C. Li, J. Hu and S. Liu, *Soft Matter*, 2012, **8**, 7096–7102.
14 S. Valdez, M. Robertson and Z. Qiang, *Macromol. Rapid Commun.*, 2022, **43**, 2200421.
15 X.-d Wang, O. S. Wolfbeis and R. J. Meier, *Chem. Soc. Rev.*, 2013, **42**, 7834–7869.
16 G. Virat, K. K. Maiti, R. B. Amal Raj and E. B. Gowd, *Soft Matter*, 2023, **19**, 6671–6682.
17 K. Okada and Y. Maeda, *J. Appl. Polym. Sci.*, 2013, **130**, 201–205.
18 J.-C. Yang, Y.-C. Ho and Y.-H. Chan, *ACS Appl. Mater. Interfaces*, 2019, **11**, 29341–29349.
19 S. Hirata, M. Vacha and T. Watanabe, *Jpn. J. Appl. Phys.*, 2010, **49**, 052501.
20 S. Kim, S.-J. Yoon and S. Y. Park, *J. Am. Chem. Soc.*, 2012, **134**, 12091–12097.
21 A. R. Clapp, I. L. Medintz, J. M. Mauro, B. R. Fisher, M. G. Bawendi and H. Mattoussi, *J. Am. Chem. Soc.*, 2004, **126**, 301–310.
22 S. Karasawa, T. Araki, T. Nagai, H. Mizuno and A. Miyawaki, *Biochem. J.*, 2004, **381**, 307–312.
23 U. Woggon, *Optical properties of semiconductor quantum dots*, Springer, 1997.
24 I. L. Medintz, S. A. Trammell, H. Mattoussi and J. M. Mauro, *J. Am. Chem. Soc.*, 2004, **126**, 30–31.
25 T. Basché, A. Bottin, C. Li, K. Müllen, J.-H. Kim, B.-H. Sohn, P. Prabhakaran and K.-S. Lee, *Macromol. Rapid Commun.*, 2015, **36**, 1026–1046.
26 A. R. Clapp, I. L. Medintz and H. Mattoussi, *ChemPhysChem*, 2006, **7**, 47–57.
27 L. Vijaya, S. Suresh, R. Patel and E. B. Gowd, *ACS Macro Lett.*, 2022, **11**, 1272–1277.
28 I. Konidakis, A. Karagiannaki and E. Stratakis, *Nanoscale*, 2022, **14**, 2966–2989.
29 T. T. Tran, K. Bray, M. J. Ford, M. Toth and I. Aharonovich, *Nat. Nanotechnol.*, 2016, **11**, 37–41.
30 Y. Xu, X. Wang, W. L. Zhang, F. Lv and S. Guo, *Chem. Soc. Rev.*, 2018, **47**, 586–625.
31 S. Nafiu, V. A. Apalangya, A. Yaya and E. B. Sabi, *Appl. Sci.*, 2022, **12**, 879.
32 S. Ghimire, A. Sivadas, K.-I. Yuyama, Y. Takano, R. Francis and V. Biju, *Nanoscale*, 2018, **10**, 13368–13374.
33 C. R. Kagan, C. B. Murray and M. G. Bawendi, *Phys. Rev. B: Condens. Matter Mater. Phys.*, 1996, **54**, 8633–8643.
34 P. Moroz, Z. Jin, Y. Sugiyama, D. A. Lara, N. Razgoniaeva, M. Yang, N. Kholmicheva, D. Khon, H. Mattoussi and M. Zamkov, *ACS Nano*, 2018, **12**, 5657–5665.
35 M. Yokouchi, Y. Chatani, H. Tadokoro, K. Teranishi and H. Tani, *Polymer*, 1973, **14**, 267–272.
36 N. S. Akhila, V. G. Krishnan, J. Parukoor Thomas and E. B. Gowd, *ACS Appl. Polym. Mater.*, 2024, **6**, 6864–6874.